PCCP

PAPER

View Article Online
View Journal | View Issue

Cite this: *Phys. Chem. Chem. Phys.*, 2023, **25**, 14736

Surface stabilisation of the high-spin state of Fe(II) spin-crossover complexes

Alejandro Martínez Serra, [a] Archit Dhingra, *[a] María Carmen Asensio, [bc] José Antonio Real [d] and Juan Francisco Sánchez Royo *[ac]

Received 23rd February 2023,
Accepted 16th May 2023

DOI: 10.1039/d3cp00863k

rsc.li/pccp

Temperature dependent X-ray photoemission spectroscopy (XPS) has been employed to examine the Fe 2p and N 1s core levels of the studied Fe(II) spin crossover (SCO) complexes of interest, namely: $Fe(phen)_2(NCS)_2$, $[Fe(3\text{-}Fpy)_2\{Ni(CN)_4\}]$, and $[Fe(3\text{-}Fpy)_2\{Pt(CN)_4\}]$. The changes in the Fe 2p core-level spectra with temperature indicate spin state transitions in these SCO complexes, which are consistent with one's expectations and the existing literature. Additionally, the temperature dependence of the binding energy of the N 1s core-level provides further physical insights into the ligand-to-metal charge transfer phenomenon in these molecules. The high-spin fraction *versus* temperature plots reveal that the surface of each of the molecules studied herein is found to be in the high-spin state at temperatures both in the vicinity of room temperature and below their respective transition temperature alike, with the stability of the high-spin state of these molecules varying with the choice of ligand.

Introduction

Fe(II) spin crossover (SCO) complexes are molecules in which the strength of the octahedral ligand field surrounding the Fe atom is in the realm where even slight external perturbations, like change of temperature[1–5] or magnetic field,[6–8] can trigger a spin-state transition in these molecules.[9–15] At low temperatures, when the octahedral ligand field splitting (Δ_{oct}) between the t_{2g} and e_g orbitals is high, the SCO complexes occupy the diamagnetic (S = 0) low-spin state (LS). However, at temperatures higher than the critical transition temperature T_c, when the Δ_{oct} between the t_{2g} and e_g orbitals is lowered, these molecules occupy the paramagnetic (S = 2) high-spin state (HS).[14,16–20] Owing to the ease with which such spin-state transitions can be achieved in the Fe(II) SCO complexes and the bistability of these spin states,[9,21,22] these molecules make great candidates for room temperature spintronics (since triggering the spin-state transition closer to room temperature is very much achievable),[23–25] and nonvolatile memory applications.[26–28] The existence of room temperature magnetic moment in these molecules may also be exploited for molecular transistor-based quantum information science applications.[29–31] While there are multiple Fe(II) SCO complexes, the model Fe(II) SCO compound $Fe(phen)_2(NCS)_2$ and the Hofmann-like Fe(II) SCO complexes have gathered quite a lot of research interest over the past two decades, in particular.[4,23,32–36]

Since Fe(II) experiences a considerable electronic change with a spin-state transition[37] (the occupancy diagram for the LS and HS electronic configurations is presented in Fig. 1a), these transitions can be easily detected by monitoring the temperature-dependent changes in the Fe 2p core-level XPS spectra of Fe(II) SCO complexes.[38–49] Therefore, in this work, we have used temperature dependent X-ray photoemission spectroscopy (XPS) to study the temperature dependence of the Fe 2p and N 1s core levels of the discrete mononuclear complex $Fe(phen)_2(NCS)_2$ (schematic shown in Fig. 1b), as well as two 2D Hofmann-like coordination polymers: $[Fe(3\text{-}Fpy)_2\{Ni(CN)_4\}]$ and $[Fe(3\text{-}Fpy)_2\{Pt(CN)_4\}]$ (a side-view of which is shown in Fig. 1c), in order to probe the spin crossover transitions in the nanocrystals of these systems. Moreover, as XPS is a surface-sensitive technique, these measurements would allow us to elucidate surface effects of the ligand-dependent variation in the stability of the high-spin state in the nanocrystals of the Fe(II) SCO complexes studied herein, which may be different from those of the bulk; hence, becoming particularly relevant in the case of the nanoparticles of these SCO complexes (which, naturally, possess significantly high surface-to-volume ratio).[12,50,51] The knowledge of the surface of the nanocrystals of each of these SCO complexes would be indispensable from the standpoint of device fabrication as, generally, surfaces and resultant interfacial

[a] *Institut de Ciència dels Materials de la Universitat de València (ICMUV), University of Valencia, Carrer del Catedrátic José Beltrán Martinez, 2, Paterna 46980, Valencia, Spain. E-mail: archit.dhingra@uv.es, Juan.F.Sanchez@uv.es*
[b] *Materials Science Institute of Madrid (ICMM/CSIC), Cantoblanco, Madrid E-28049, Spain*
[c] *MATINÉE, the CSIC Associated Unit between the Materials Science Institute (ICMUV) and the ICMM, Cantoblanco, Madrid E-28049, Spain*
[d] *Institut de Ciència Molecular (ICMol), University of Valencia, Carrer del Catedrátic José Beltrán Martinez, 2, Paterna 46980, Valencia, Spain*

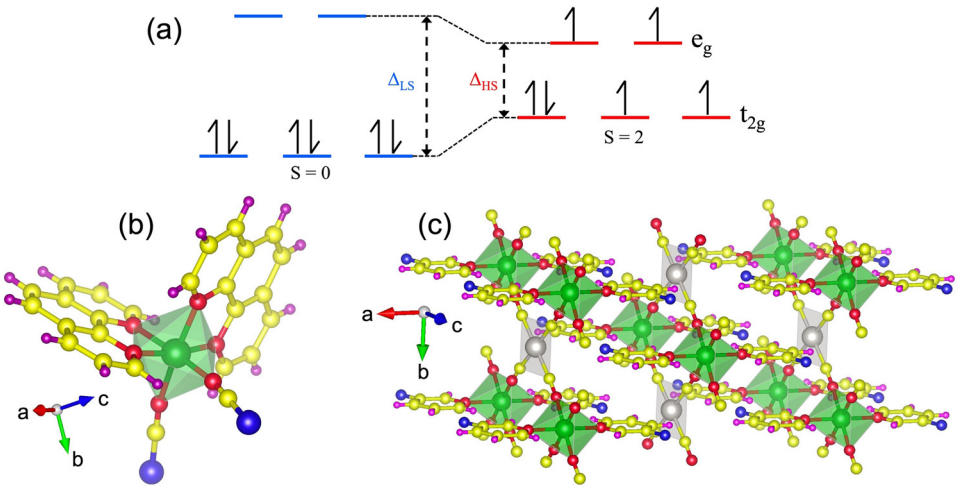

Fig. 1 (a) [Ar]3d^6 electronic configuration in an octahedral ligand field of the Fe(II) ion in the LS and HS states, and ball-and-stick models of (b) $Fe(phen)_2(NCS)_2$ and (c) the Hofmann-like Fe(II) SCO complexes, respectively. Atom codes for Fig. 1b: Fe (green); N (red); C (yellow); S (blue); H (purple). Atom codes for Fig. 1c: Fe (green); Ni/Pt (silver); N (red); C (yellow); F (blue); H (purple).

interactions are well-known to have strong influence on the device properties of a material.[52–55]

Experimental details

The nanocrystals of $Fe(phen)_2(NCS)_2$, $[Fe(3\text{-}Fpy)_2\{Ni(CN)\}_4]$ and $[Fe(3\text{-}Fpy)_2\{Pt(CN)\}_4]$ complexes were prepared according to the methods reported previously.[12,56]

Temperature dependent XPS measurements were used to study the temperature-dependent evolution of spin-state occupancy in $Fe(phen)_2(NCS)_2$, $[Fe(3\text{-}Fpy)_2\{Ni(CN)_4\}]$, and $[Fe(3\text{-}Fpy)_2\{Pt(CN)_4\}]$. XPS measurements were performed in a SPECS GmbH system (base pressure 1.0×10^{-10} mbar) equipped with a PHOIBOS 150 2D-CMOS hemispherical analyser. Photoelectrons were excited with the Al-Kα line (1,486.7 eV) of a monochromatic X-ray source μ-FOCUS 500 (SPECS GmbH). Measurements were taken with a pass-energy of 20 eV.

Results and discussion

Temperature dependent photoemission spectra of the Fe 2p core-level of the nanocrystals of $Fe(phen)_2(NCS)_2$, $[Fe(3\text{-}Fpy)_2\{Ni(CN)_4\}]$, and $[Fe(3\text{-}Fpy)_2\{Pt(CN)_4\}]$ are shown in Fig. 2. The XPS spectra of the Fe 2p core-level of $Fe(phen)_2(NCS)_2$ collected for a set of temperatures ranging from 113–270 K are shown in Fig. 2a. Likewise, the photoemission spectra of the Fe 2p

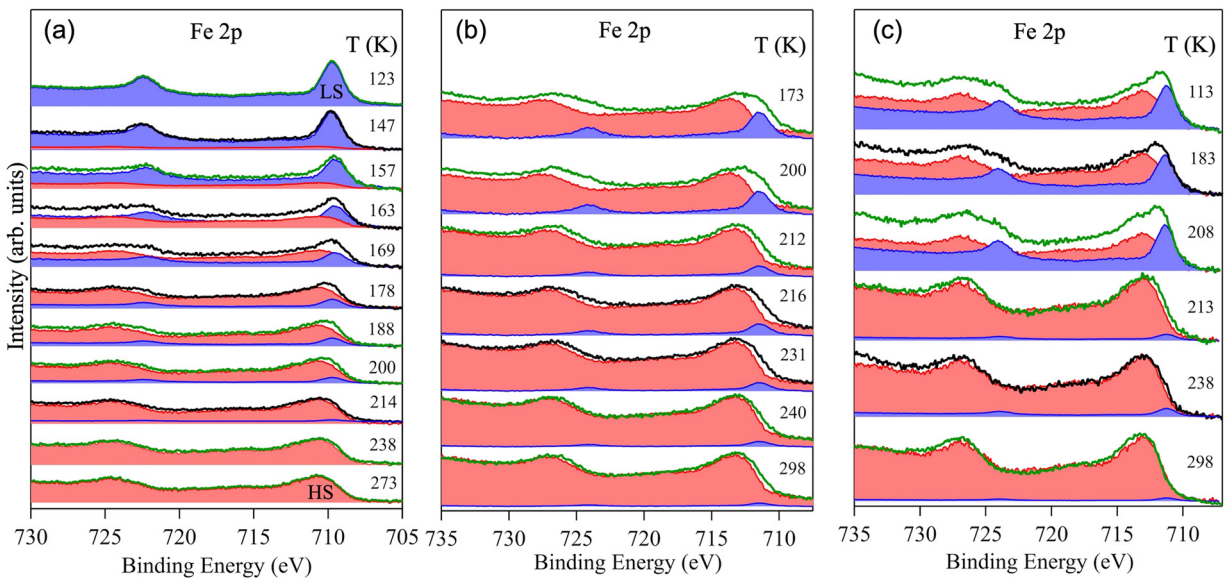

Fig. 2 Temperature dependent XPS of the Fe 2p core-level of (a) $Fe(phen)_2(NCS)_2$, (b) $[Fe(3\text{-}Fpy)_2\{Ni(CN)\}_4]$, and (c) $[Fe(3\text{-}Fpy)_2\{Pt(CN)\}_4]$. The raw spectra in green depict lowering of temperature while the ones in black represent increase in temperature. The fits in blue indicate the LS, and the fits in red represent the HS.

core-level of $[Fe(3\text{-}Fpy)_2\{Ni(CN)_4\}]$ (Fig. 2b) and $[Fe(3\text{-}Fpy)_2\{Pt(CN)_4\}]$ (Fig. 2c) were recorded over a temperature range of 113–298 K and 173–298 K, respectively. Since an increase in temperature would translate to the elongation of Fe–N bonds and weakening of the ligand-to-metal charge transfer (LMCT), the HS electronic configuration for each of the studied systems is assigned the XPS peak at a higher binding energy value in comparison with the XPS peak representing the respective LS electronic configuration. Such an assignment of the XPS peaks is consistent with the elevated effective nuclear charge experienced by the Fe 2p electrons in the HS configuration, and the existing literature.[38–49]

An energy difference in excess of 1 eV between the XPS peaks of the LS and HS configurations, is consistent with the energy difference between these configurations reported previously.[14,57,58] Thus, the value of the energy difference between the LS and HS electronic configurations of these SCO complexes, along with their respective structural symmetry (see Fig. 1b and c), confirm that these compounds are Fe(II) SCO complexes indeed. It is to be noted that the information provided by these measurements is unaffected by the fact that the temperature ranges over which the XPS spectra of the Fe 2p core levels of these materials were taken are not all the same, since the chosen temperature ranges cover the spin-crossover region for each of the studied systems.

Temperature-dependent variations in the photoemission spectra of the N 1s core-level of $Fe(phen)_2(NCS)_2$, $[Fe(3\text{-}Fpy)_2\{Ni(CN)_4\}]$, and $[Fe(3\text{-}Fpy)_2\{Pt(CN)_4\}]$ are shown in Fig. 3. Based on the peak ratios of the fitted N 1s core-level components, and the LMCT arguments, it is clear that the N 1s features with greater peak areas and higher binding energies correspond to the nitrogen atoms in "phen" (in Fig. 3a), "$Ni(CN)_4$" (in Fig. 3b) and "$Pt(CN)_4$" (in Fig. 3c), respectively. In Fig. 3a, the peak of the N 1s core-level component at the higher binding energy (N2) shifts towards even higher values as $Fe(phen)_2(NCS)_2$ is cooled down to 113 K. Such a temperature dependent change in the binding energy of the N2 component agrees with the temperature-driven shortening of the Fe–N bond lengths. Moreover, no observable change in the binding energy of the N 1s feature at the lower binding energy (N1) implies that more charge is transferred between N2 and Fe than between N1 and Fe. On the other hand, as can be seen from Fig. 3b and c, there are no discernible changes in the binding energies of either of the N 1s core-level components of the studied Hofmann-like SCO complexes (*viz.*, $[Fe(3\text{-}Fpy)_2\{Ni(CN)_4\}]$ and $[Fe(3\text{-}Fpy)_2\{Pt(CN)_4\}]$). Lack of identifiable temperature-driven shifts in the binding energies of both the N 1s core-level components of these Hofmann-like complexes indicates that their respective HS electronic configuration are quite stable in comparison with the HS electronic configuration of $Fe(phen)_2(NCS)_2$. In other words, the HS electronic configurations of $[Fe(3\text{-}Fpy)_2\{Ni(CN)_4\}]$ and $[Fe(3\text{-}Fpy)_2\{Pt(CN)_4\}]$ are somewhat more immune to thermal fluctuations than the HS electronic configuration of $Fe(phen)_2(NCS)_2$.

A closer look into the XPS spectra of the Fe 2p and N 1s core levels, shown in Fig. 2 and 3 respectively, provides further physical insights into the nature of the Fe–N1 bonds of all the materials studied herein. To elaborate further, the binding energies of both the LS and HS electronic configurations of $Fe(phen)_2(NCS)_2$ (Fig. 2a) are lower than that of the respective binding energies of the LS and HS electronic configurations of the Hofmann-like complexes (Fig. 2b and 2c); however, while the binding energy of the N2 feature, of the N 1s core-level, of each of these complexes is (more or less) the same, the binding energy of the N1 feature of $Fe(phen)_2(NCS)_2$ (Fig. 3a) is higher than the binding energies of the N1 features of the Hofmann-like complexes (Fig. 3b and 3c). This observation is consistent

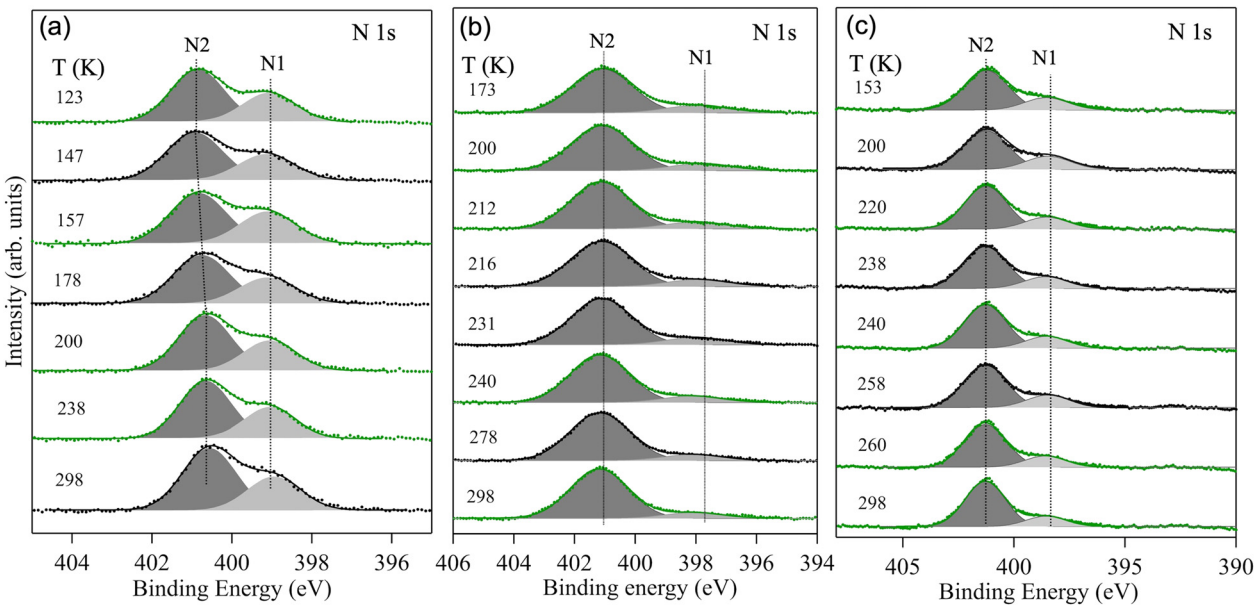

Fig. 3 Temperature dependent XPS of the N 1s core-level of (a) $Fe(phen)_2(NCS)_2$, (b) $[Fe(3\text{-}Fpy)_2\{Ni(CN)\}_4]$, and (c) $[Fe(3\text{-}Fpy)_2\{Pt(CN)\}_4]$. As in Fig. 2, the raw spectra in green depict lowering of temperature while the ones in black represent increase in temperature.

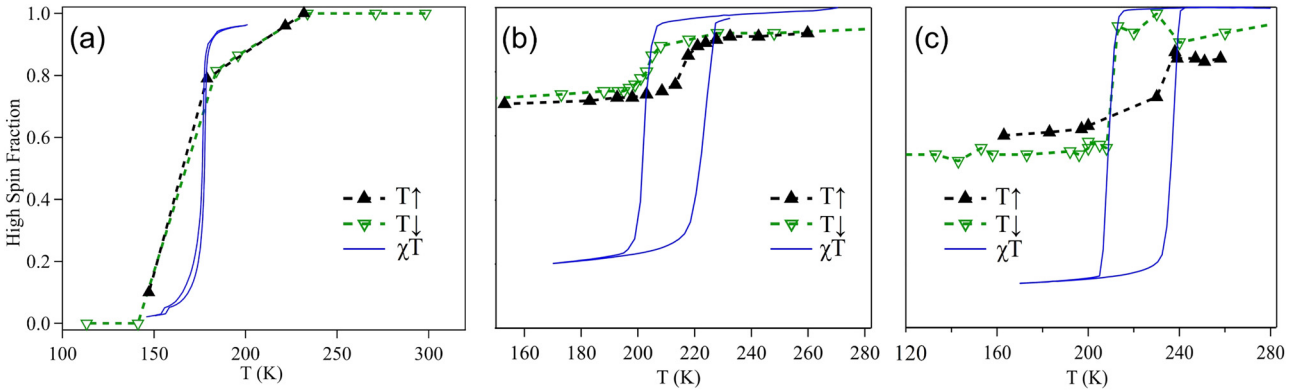

Fig. 4 High-spin fractions of (a) $Fe(phen)_2(NCS)_2$, (b) $[Fe(3\text{-}Fpy)_2\{Ni(CN)\}_4]$, and (c) $[Fe(3\text{-}Fpy)_2\{Pt(CN)\}_4]$ as a function of temperature. Solid black and hollow green triangles represent the data points collected from the XPS measurements. Blue curves show the normalised experimental thermal hysteresis for each of the studied molecule, as extracted from ref. 56, 59, and they are included here to draw a comparison with the results of our XPS measurements.

with the fact that since the electronegativity of fluorine (in 3-Fpy) is higher than the electronegativity of sulphur (in NCS), the extent of electron transfer from Fe to the "3-Fpy" group should be greater than the extent of electron transfer from Fe to the "NCS" group. Hence, the apparent differences in the binding energies of the respective components of the Fe 2p and N 1s core levels, shown in Fig. 2 and 3 respectively, quite clearly convey that the Fe–N1 bonds in the Hofmann-like complexes are stronger (or more ionic) than the Fe–N1 bonds in $Fe(phen)_2(NCS)_2$.

The quantification of high-spin state occupancy in these systems is achieved by extracting the LS and HS peak areas from the temperature dependent XPS of the Fe 2p core-level of these materials (Fig. 2) and then plotting the high-spin fractions of these molecules as a function of temperature, as shown in Fig. 4. Upon comparing the temperature dependence of the high-spin fractions of $Fe(phen)_2(NCS)_2$ extrapolated from the XPS measurements with the ones obtained from the magnetic susceptibility measurements[56] (shown in Fig. 4a), a strong agreement between the two is observed. Therefore, it is fair to claim that XPS, indeed, serves as a promising tool to monitor spin transitions and cooperative effects in the SCO complexes.

However, a similar comparison drawn between the XPS measurements and the magnetic susceptibility measurements taken on the each of the Hofmann-like SCO systems[59] (Fig. 4b and c) reveals that there lies a caveat. The caveat, stemming from the fact that XPS is a highly surface sensitive technique, is that an observed disagreement between the two kinds of measurements is not something to be frowned upon as it would imply that the surface of each of the studied Hofmann-like SCO systems is different from its bulk. That is to say, the HS tends to stabilise at the surface of the Hofmann-like SCO molecules studied herein even at temperatures well below that of the transition temperatures for the whole molecule. This fact can be attributed to a steric inhibition of the Fe(II) coordination environment dictating the extent of the SCO transition, as has been observed in other systems,[60,61] which clearly correlates with the lack of energy shift of the N 1s core level that is observed in the studied Hofmann-like SCO complexes (refer to Fig. 3b and c). Besides, the fact that a complete HS-LS spin transition is seen in the $Fe(phen)_2(NCS)_2$ molecular system unlike the incomplete transition in the Hofmann-like SCO complexes seems to be a consequence of the intrinsic long-range nature of the magnetic super-exchange interaction J, which plays a crucial role in driving the cooperativity in the Hofmann-like SCO complexes,[62] and is naturally limited at the surface of these systems due to the breaking of the spatial translation symmetry of the bulk.

Conclusions

In conclusion, temperature-dependent XPS is employed to gain further physical insights into the spin-state transitions in the nanocrystals of $Fe(phen)_2(NCS)_2$, $[Fe(3\text{-}Fpy)_2\{Ni(CN)_4\}]$, and $[Fe(3\text{-}Fpy)_2\{Pt(CN)_4\}]$. Changes in the Fe 2p core-level spectra as a consequence of varying temperature clearly evidences spin state transitions in these SCO complexes, which are consistent with one's expectations and the existing literature. Furthermore, the temperature dependence of the binding energy of the N 1s core-level of $Fe(phen)_2(NCS)_2$ signifies that more charge is transferred between N2 (the nitrogen atoms in "phen") and Fe than between N1 (the nitrogen atoms in "NCS") and Fe. The high-spin fractions of $Fe(phen)_2(NCS)_2$ extrapolated from the XPS measurements are found to be in great agreement with the results of the existing magnetic susceptibility measurements, whereas drawing similar comparison between the temperature-dependent XPS and the magnetic susceptibility measurements taken on the each of the two Hofmann-like SCO systems would be naïve and, therefore, requires special attention (due to the reasons discussed above). Nevertheless, it is revealed that: (i) all the molecules studied herein are found to be in the high-spin state at room temperature and (ii) the high-spin state stability of these molecules varies with the choice of ligand. Overall, it is worth mentioning that high values of room-temperature HS occupancy especially

at the surface of the nanocrystals of these molecules, and their great immunity to thermal fluctuations, opens new pathways for room-temperature spintronics and quantum information science applications.

Author contributions

JFSR conceived the idea and coordinated this work. JAR supervised the sample preparation and structural implications of photoemission results. AMS performed photoemission measurements and MCA, AD, and JFSR analysed and interpreted experimental results. AD, MCA, and JFSR co-wrote the manuscript, with inputs from all authors. All authors have given approval to the final version of the manuscript.

Conflicts of interest

The authors declare that they have no known competing financial interests or personal relationships that could have appeared to influence the work reported in this paper.

Acknowledgements

This work was made possible by the Advanced Materials programme and was supported by the MCIN with funding from European Union NextGenerationEU (PRTR-C17.I1) and by Generalitat Valenciana (Project MFA/2022/009). Support from the PROMETEO program of the Generalitat Valenciana (project PROMETEU/2021/082), which is part of the Agencia Estatal de Investigación, funded by the Project PID2020-112507GB-I00 funded by MCIN/AEI/10.13039/501100011033. The present research has been undertaken in the context of the Associated Research Unit MATINÉE of the CSIC (Spanish Scientific Research Council), created between the Institute of Materials Science (ICMUV) of Valencia University and the Materials Science Institute of Madrid (ICMM). The authors acknowledge financial support from the MIG-20201021 LION-HD project. The Research Funds of the Valencian Community, through the project PROMETEO/2020/091. Also, the project MAT2020 NIRVANA (PID2020-119628RB-C32) financed by the Ministry of Science and Innovation, Government of Spain. Finally, the present work has also been supported by the project INGENIOUS (TED2021-132656B-C21 & TED2021-132656B-C22) granted by the Call 2021 – ''Ecological Transition and Digital Transition Projects'' promoted by the Ministry of Science and Innovation, funded by the European Union within the ''NextGeneration'' EU program, the Recovery, Transformation, and Resilience Plan, and the State Investigation Agency.

Notes and references

1 B. Warner, J. C. Oberg, T. G. Gill, F. El Hallak, C. F. Hirjibehedin, M. Serri, S. Heutz, M.-A. Arrio, P. Sainctavit, M. Mannini, G. Poneti, R. Sessoli and P. Rosa, *J. Phys. Chem. Lett.*, 2013, **4**, 1546–1552.
2 S. Rohlf, M. Gruber, B. M. Flöser, J. Grunwald, S. Jarausch, F. Diekmann, M. Kalläne, T. Jasper-Toennies, A. Buchholz, W. Plass, R. Berndt, F. Tuczek and K. Rossnagel, *J. Phys. Chem. Lett.*, 2018, **9**, 1491–1496.
3 G. Hao, A. Mosey, X. Jiang, A. J. Yost, K. R. Sapkota, G. T. Wang, X. Zhang, J. Zhang, A. T. N'Diaye, R. Cheng, X. Xu and P. A. Dowben, *Appl. Phys. Lett.*, 2019, **114**, 032901.
4 J. A. Real, A. B. Gaspar and M. C. Muñoz, *Dalton Trans.*, 2005, 2062.
5 X. Zhang, S. Mu, G. Chastanet, N. Daro, T. Palamarciuc, P. Rosa, J.-F. Létard, J. Liu, G. E. Sterbinsky, D. A. Arena, C. Etrillard, B. Kundys, B. Doudin and P. A. Dowben, *J. Phys. Chem. C*, 2015, **119**, 16293–16302.
6 M. Salimi, S. Fathizadeh and S. Behnia, *Phys. Scr.*, 2022, **97**, 055005.
7 G. Hao, A. T. N'Diaye, T. K. Ekanayaka, A. S. Dale, X. Jiang, E. Mishra, C. Mellinger, S. Yazdani, J. W. Freeland, J. Zhang, R. Cheng, X. Xu and P. A. Dowben, *Magnetochemistry*, 2021, **7**, 135.
8 X. Zhang, P. S. Costa, J. Hooper, D. P. Miller, A. T. N'Diaye, S. Beniwal, X. Jiang, Y. Yin, P. Rosa, L. Routaboul, M. Gonidec, L. Poggini, P. Braunstein, B. Doudin, X. Xu, A. Enders, E. Zurek and P. A. Dowben, *Adv. Mater.*, 2017, **29**, 1702257.
9 M. Sorai and S. Seki, *J. Phys. Chem. Solids*, 1974, **35**, 555–570.
10 H. A. Goodwin, *Coord. Chem. Rev.*, 1976, **18**, 293–325.
11 M. Reiher, *Inorg Chem.*, 2002, **41**, 6928–6935.
12 V. Martínez, I. Boldog, A. B. Gaspar, V. Ksenofontov, A. Bhattacharjee, P. Gütlich and J. A. Real, *Chem. Mater.*, 2010, **22**, 4271–4281.
13 M. C. Muñoz and J. A. Real, *Coord. Chem. Rev.*, 2011, **255**, 2068–2093.
14 M. Gruber, T. Miyamachi, V. Davesne, M. Bowen, S. Boukari, W. Wulfhekel, M. Alouani and E. Beaurepaire, *J. Chem. Phys.*, 2017, **146**, 092312.
15 N. A. A. M. Amin, S. M. Said, M. F. M. Salleh, A. M. Afifi, N. M. J. N. Ibrahim, M. M. I. M. Hasnan, M. Tahir and N. Z. I. Hashim, *Inorg. Chim. Acta*, 2023, **544**, 121168.
16 T. Granier, B. Gallois, J. Gaultier, J. A. Real and J. Zarembowitch, *Inorg. Chem.*, 1993, **32**, 5305–5312.
17 P. Gütlich, *Metal Complexes*, Springer Berlin Heidelberg, Berlin, Heidelberg, 2007, pp. 83–195.
18 G. Bradley, V. McKee, S. M. Nelson and J. Nelson, *J. Chem. Soc., Dalton Trans.*, 1978, 522–526.
19 Y. Zhang, *J. Chem. Phys.*, 2019, **151**, 134701.
20 T. K. Ekanayaka, K. P. Maity, B. Doudin and P. A. Dowben, *Nanomaterials*, 2022, **12**, 1742.
21 E. König and K. Madeja, *Chem. Commun.*, 1966, 61–62.
22 X. Jiang, G. Hao, X. Wang, A. Mosey, X. Zhang, L. Yu, A. J. Yost, X. Zhang, A. D. DiChiara, A. T. N'Diaye, X. Cheng, J. Zhang, R. Cheng, X. Xu and P. A. Dowben, *J. Phys.: Condens. Matter*, 2019, **31**, 315401.
23 F. J. Valverde-Muñoz, A. B. Gaspar, S. I. Shylin, V. Ksenofontov and J. A. Real, *Inorg. Chem.*, 2015, **54**, 7906–7914.
24 Y. Zhang, *J. Chem. Phys.*, 2020, **153**, 134704.
25 S. V. Aradhya and L. Venkataraman, *Nat. Nanotechnol.*, 2013, **8**, 399–410.

26 A. Mosey, A. S. Dale, G. Hao, A. N'Diaye, P. A. Dowben and R. Cheng, *J. Phys. Chem. Lett.*, 2020, **11**, 8231–8237.
27 T. K. Ekanayaka, G. Hao, A. Mosey, A. S. Dale, X. Jiang, A. J. Yost, K. R. Sapkota, G. T. Wang, J. Zhang, A. T. N'Diaye, A. Marshall, R. Cheng, A. Naeemi, X. Xu and P. A. Dowben, *Magnetochemistry*, 2021, **7**, 37.
28 K. S. Kumar and M. Ruben, *Angew. Chem., Int. Ed.*, 2021, **60**, 7502–7521.
29 G. Hao, R. Cheng and P. A. Dowben, *J. Phys.: Condens. Matter*, 2020, **32**, 234002.
30 G. Hao, A. S. Dale, A. T. N'Diaye, R. V. Chopdekar, R. J. Koch, X. Jiang, C. Mellinger, J. Zhang, R. Cheng, X. Xu and P. A. Dowben, *J. Phys.: Condens. Matter*, 2022, **34**, 295201.
31 A. Dhingra, X. Hu, M. F. Borunda, J. F. Johnson, C. Binek, J. Bird, A. T. N'Diaye, J.-P. Sutter, E. Delahaye, E. D. Switzer, E. del Barco, T. S. Rahman and P. A. Dowben, *J. Phys.: Condens. Matter*, 2022, **34**, 441501.
32 F. J. Valverde-Muñoz, M. Seredyuk, M. C. Muñoz, K. Znovjyak, I. O. Fritsky and J. A. Real, *Inorg. Chem.*, 2016, **55**, 10654–10665.
33 L. Piñeiro-López, F. J. Valverde-Muñoz, M. Seredyuk, C. Bartual-Murgui, M. C. Muñoz and J. A. Real, *Eur. J. Inorg. Chem.*, 2018, 289–296.
34 S. I. Shylin, O. I. Kucheriv, S. Shova, V. Ksenofontov, W. Tremel and I. A. Gural'skiy, *Inorg. Chem.*, 2020, **59**, 6541–6549.
35 T. Kosone, R. Kosuge, M. Tanaka, T. Kawasaki and N. Adachi, *New J. Chem.*, 2022, **46**, 10540–10544.
36 G. Agustí, R. Ohtani, K. Yoneda, A. B. Gaspar, M. Ohba, J. F. Sánchez-Royo, M. C. Muñoz, S. Kitagawa and J. A. Real, *Angew. Chem.*, 2009, **121**, 9106–9109.
37 K. S. Murray, *Spin-Crossover Materials*, John Wiley & Sons Ltd, Oxford, UK, 2013, pp. 1–54.
38 K. Burger, C. Furlani and G. Mattogno, *J. Electron Spectrosc. Relat. Phenom.*, 1980, **21**, 249–256.
39 K. Burger, H. Ebel and K. Madeja, *J. Electron Spectrosc. Relat. Phenom.*, 1982, **28**, 115–121.
40 T. K. Ekanayaka, H. Kurz, K. A. McElveen, G. Hao, E. Mishra, A. T. N'Diaye, R. Y. Lai, B. Weber and P. A. Dowben, *Phys. Chem. Chem. Phys.*, 2022, **24**, 883–894.
41 A. Pronschinske, R. C. Bruce, G. Lewis, Y. Chen, A. Calzolari, M. Buongiorno-Nardelli, D. A. Shultz, W. You and D. B. Dougherty, *Chem. Commun.*, 2013, **49**, 10446.
42 S. Beniwal, S. Sarkar, F. Baier, B. Weber, P. A. Dowben and A. Enders, *J. Phys.: Condens. Matter*, 2020, **32**, 324003.
43 J.-Y. Son, K. Takubo, D. Asakura, J. W. Quilty, T. Mizokawa, A. Nakamoto and N. Kojima, *J. Phys. Soc. Jpn.*, 2007, **76**, 084703.
44 L. Poggini, G. Londi, M. Milek, A. Naim, V. Lanzilotto, B. Cortigiani, F. Bondino, E. Magnano, E. Otero, P. Sainctavit, M.-A. Arrio, A. Juhin, M. Marchivie, M. M. Khusniyarov, F. Totti, P. Rosa and M. Mannini, *Nanoscale*, 2019, **11**, 20006–20014.
45 L. Li, S. M. Neville, A. R. Craze, J. K. Clegg, N. F. Sciortino, K. S. A. Arachchige, O. Mustonen, C. E. Marjo, C. R. McRae, C. J. Kepert, L. F. Lindoy, J. R. Aldrich-Wright and F. Li, *ACS Omega*, 2017, **2**, 3349–3353.
46 S. Beniwal, X. Zhang, S. Mu, A. Naim, P. Rosa, G. Chastanet, J.-F. Létard, J. Liu, G. E. Sterbinsky, D. A. Arena, P. A. Dowben and A. Enders, *J. Phys.: Condens. Matter*, 2016, **28**, 206002.
47 E. C. Ellingsworth, B. Turner and G. Szulczewski, *RSC Adv.*, 2013, **3**, 3745.
48 A. P. Grosvenor, B. A. Kobe, M. C. Biesinger and N. S. McIntyre, *Surf. Interface Anal.*, 2004, **36**, 1564–1574.
49 A. R. Craze, C. E. Marjo and F. Li, *Dalton Trans.*, 2022, **51**, 428–441.
50 J. R. Galán-Mascarós, E. Coronado, A. Forment-Aliaga, M. Monrabal-Capilla, E. Pinilla-Cienfuegos and M. Ceolin, *Inorg. Chem.*, 2010, **49**, 5706–5714.
51 R. Torres-Cavanillas, M. Morant-Giner, G. Escorcia-Ariza, J. Dugay, J. Canet-Ferrer, S. Tatay, S. Cardona-Serra, M. Giménez-Marqués, M. Galbiati, A. Forment-Aliaga and E. Coronado, *Nat. Chem.*, 2021, **13**, 1101–1109.
52 A. Dhingra, D. Sando, P.-S. Lu, Z. G. Marzouk, V. Nagarajan and P. A. Dowben, *J. Appl. Phys.*, 2021, **130**, 025304.
53 Y. Bai, X. Meng and S. Yang, *Adv. Energy Mater.*, 2018, **8**, 1701883.
54 H. Zhang, Y. Li, X. Zhang, Y. Zhang and H. Zhou, *Mater. Chem. Front.*, 2020, **4**, 2863–2880.
55 A. Dhingra, D. E. Nikonov, A. Lipatov, A. Sinitskii and P. A. Dowben, *J. Mater. Res.*, 2023, **38**, 52–68.
56 B. Gallois, J. A. Real, C. Hauw and J. Zarembowitch, *Inorg. Chem.*, 1990, **29**, 1152–1158.
57 V. Briois, C. Ch dit Moulin, Ph Sainctavit, Ch Brouder and A.-M. Flank, *J. Am. Chem. Soc.*, 1995, **117**, 1019–1026.
58 C. Cartier dit Moulin, P. Rudolf, A. M. Flank and C. Te Chen, *J. Phys. Chem.*, 1992, **96**, 6196–6198.
59 V. Martínez, A. B. Gaspar, M. C. Muñoz, G. V. Bukin, G. Levchenko and J. A. Real, *Chem. – Eur. J.*, 2009, **15**, 10960–10971.
60 J. M. Holland, S. A. Barrett, C. A. Kilner and M. A. Halcrow, *Inorg. Chem. Commun.*, 2002, **5**, 328–332.
61 A. R. Craze, M. M. Bhadbhade, Y. Komatsumaru, C. E. Marjo, S. Hayami and F. Li, *Inorg. Chem.*, 2020, **59**, 1274–1283.
62 H. Banerjee, M. Kumar and T. Saha-Dasgupta, *Phys. Rev. B*, 2014, **90**, 174433.